

# Stopped-Flow Kinetics of Tetrazine Cycloadditions; Experimental and Computational Studies toward Sequential Transition States<sup>†</sup>

Dhandapani V. Sadasivam,<sup>‡</sup> Edamana Prasad,<sup>§</sup> Robert A. Flowers, II,<sup>§</sup> and David M. Birney<sup>\*,‡</sup>

Department of Chemistry and Biochemistry, Texas Tech University, Lubbock, Texas 79409-1061 and  
Department of Chemistry, Lehigh University, Bethlehem, Pennsylvania 18015

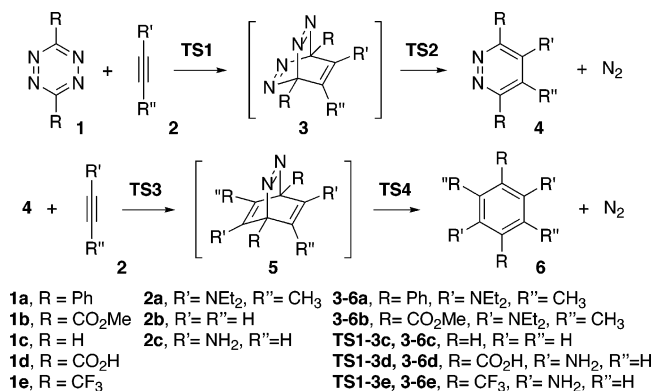
Received: June 23, 2005; In Final Form: August 6, 2005

The Diels–Alder cycloadditions of tetrazines (**1**) with alkynes (**2**) are expected to give bicyclic adducts (**3**). Kinetic measurements of the cycloadditions of **1a** and **1b** with **2a** give  $\Delta G^\ddagger = 19.2 \pm 1.0$  and  $11.5 \pm 1.2$  kcal/mol, respectively. Stopped-flow UV studies on the reaction of **1b** with **2a** show an isosbestic point at 428 nm; this places an upper limit of  $11.6 \pm 2.6$  kcal/mol on  $\Delta G^\ddagger$  for loss of N<sub>2</sub> from the putative bicyclic intermediate **3b**. Calculations (B3LYP/6-31G(d,p) + ZPVE) of transition structures for the reaction of tetrazinediacid **1d** with propynylamine **2c** are consistent with the experimental results for the reaction of **1b** with **2a**. This and several related model systems reveal two interesting features of the calculated energy surfaces. First, there may be no barrier for the loss of nitrogen from structures **3** and thus there may be two sequential transition states. This also extends Berson's correlation of activation energy with reaction energy in pericyclic reactions to significantly lower barriers. Second, for the cycloaddition of **4e** and **2c**, there is neither an intermediate nor a transition state between **TS3e** and the final product **6e**. It appears that the energy surface "turns a corner" in the vicinity of a structure resembling **5e**. This is not a mathematically well-defined point but has chemical consequences in that the overall exothermicity of the reaction from **4e** to **6e** is not felt in **TS3e**.

## Introduction

1,2,4,5-Tetrazines (**1**) and pyridazines (**4**) are well-known to act as electron deficient dienes in inverse electron demand Diels–Alder reactions<sup>1</sup> with electron-rich dienophiles such as alkynes. They are useful for the synthesis of highly substituted pyridazines, other heterocycles, and benzenes as well as in the preparation of rigid molecular receptors.<sup>1</sup> Trends in reactivity of tetrazines have been explored in some detail by Boger and co-workers.<sup>1h</sup> The expected bicyclic intermediates (e.g., **3** and **5**, Scheme 1) have never been observed; the only products (e.g., **4** and **6**) arise from loss of nitrogen. This is not particularly surprising as the deazetization of **3** and **5** should be quite exothermic and could occur via an allowed retro-Diels–Alder reaction. Indeed, it is often found that exothermicities and rates are correlated for simple reaction steps.<sup>2</sup> Berson has shown a quantitative correlation for an extensive series of endothermic and moderately exothermic pericyclic reactions.<sup>3</sup> When the dienophile is an alkyne (e.g., **2**), then deazetization also forms an aromatic ring. The question then arises—does the barrier for such an extremely exothermic reaction rise again, in line with Marcus theory,<sup>4</sup> or does it vanish as Berson's correlation suggests? In the latter case, the energy surface for the reaction of a tetrazine (**1**) with an alkyne (**2**, Scheme 1) might be very interesting. If there is no barrier for the loss of nitrogen, and since there are two nitrogens, the surface is downhill in two directions, hence it is a transition state. This suggests that there are two sequential transition states, the first for the Diels–Alder between the alkyne and the tetrazine and the second for the

## SCHEME 1: Conventional Reaction Sequence for a Tetrazine (**1**) with an Alkyne (**2**), Assuming the Intermediacy of **3** and **5**



formal substitution of N<sub>2</sub> in **4** by another N<sub>2</sub>. Such a potential energy surface is illustrated in Figure 1.

On an energy surface, it is common to find that one transition state connects one reactant (or intermediate) to one product (or intermediate).<sup>5</sup> At this point, a careful distinction needs to be made between the transition state, which reflects the statistical mechanical contributions to the energy, and the transition structure (TS), which is located by calculations on the Born–Oppenheimer potential energy surface. Recently, there has been considerable computational interest in reactions in which the intrinsic reaction coordinate (IRC)<sup>6</sup> from one transition structure connects directly to another transition structure.<sup>7–10</sup> Such reactions are characterized by a valley–ridge inflection (VRI) point on the IRC between the two TS's.<sup>7</sup> Significant computational attention has been focused on the deazetization of 2,3-diaza[2.2.1]bicyclohept-2-ene, prompted by Carpenter's seminal

<sup>†</sup> Part of the special issue "William Hase Festschrift".

\* Corresponding author e-mail: david.birney@ttu.edu.

<sup>‡</sup> Texas Tech University.

<sup>§</sup> Lehigh University.

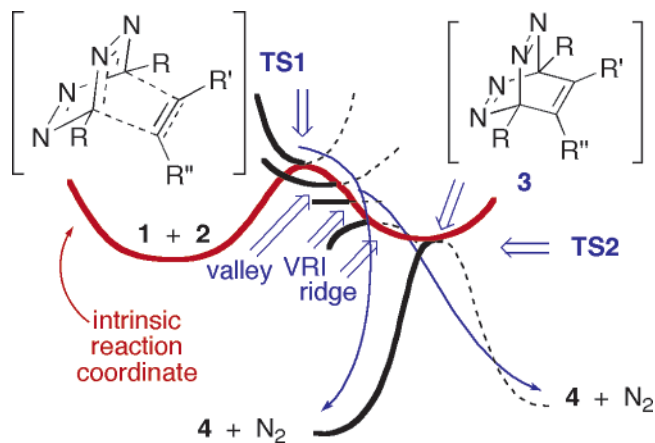
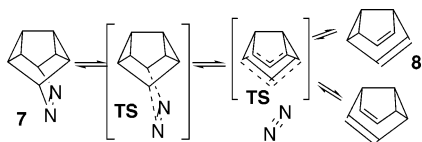
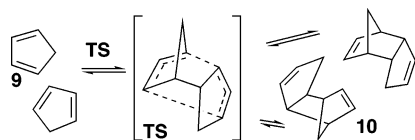


**Figure 1.** Two-dimensional energy surface for a reaction of **1** with **2**, assuming two sequential transition states (i.e., **3** is the same as TS2). Past the VRI point<sup>7</sup> the IRC<sup>6</sup> (in red) continues to the second transition state, but the steepest descent (in blue) leads directly to products.

## SCHEME 2



## SCHEME 3



work.<sup>8</sup> We have reported computational examples as well,<sup>9a,f</sup> for example, the TS for deazetization of **7** leads directly to the TS for the Cope rearrangement of semibullvalene (**8**, Scheme 2).<sup>9f</sup> Caramella et al. recently calculated that the dimerization of cyclopentadiene (**9**) proceeds via sequential Diels–Alder and Cope transition structures (Scheme 3). This and related reactions were described as “bis-pericyclic” reactions.<sup>10</sup> In all these systems, the first transition structure has some symmetry, and the second TS breaks the symmetry.

Thus the simple question—how low is the barrier for the deazetization of **3**?—takes on broader significance; a non-existent barrier means that the overall reaction proceeds via sequential transition structures. While most studies of sequential transition structures and VRIs have been computational, the tetrazine system (Scheme 1) lends itself to experimental studies that bear on this question. A straightforward method for preparation of **3** is the Diels–Alder reaction of a tetrazine (**1**) with an alkyne (**2**). Because tetrazines are strongly colored, the kinetics of such a reaction can readily be followed by UV–Vis methods; the presence of an isosbestic point is a classic test for the absence of a detectable intermediate. If the lifetime of **3** is too short for it to be detected, the kinetics puts an upper limit on its lifetime and on the barrier for the loss of nitrogen. Clearly, then, a fast initial Diels–Alder reaction is desirable because it would provide a more restrictive test of whether **3** exists or not. The Diels–Alder cycloaddition of **1b** with **2a** is particularly fast and was monitored using a stopped-flow spectrophotometer. Density functional theory (DFT) calculations were performed on model systems to complement the experiments.

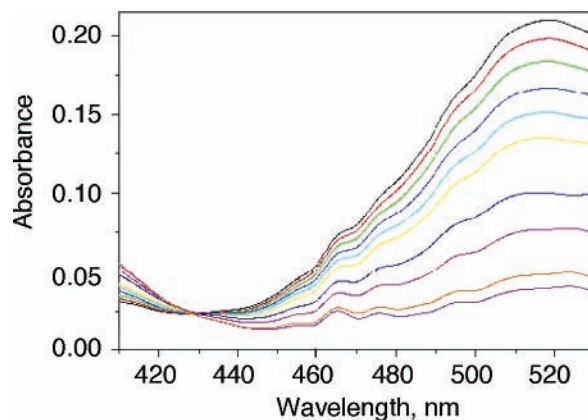
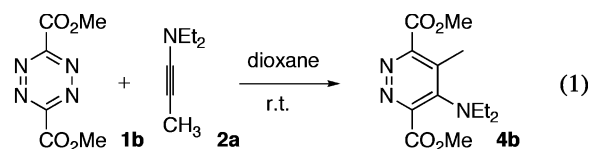


**Figure 2.** Time evolution of the absorption spectra when a 1:1 ratio of tetrazine diester (**1b**) vs ynamine (**2a**) were reacted at 15 °C. Both reagents were  $3.1 \times 10^{-3}$  M in dioxane after mixing in the stopped-flow spectrometer. Spectra were recorded at 5, 6, 8, 10, 12, 15, 25, 38, 75, and 100 ms.

## Results and Discussion

**Preliminary Studies.** Initially, commercially available diphenyltetrazine (**1a**) was reacted with the electron rich alkyne *N,N*-diethyl-1-propynylamine<sup>1c,h</sup> (**2a**) in dioxane/acetonitrile (5:1) solvent mixture, which gave pyridazine **4a**. This reaction was conveniently monitored at room temperature in a UV–Vis spectrophotometer. This clearly showed an isosbestic point at 448 nm. Under pseudo-first-order conditions, with **2a** in excess, the absorbance of tetrazine **1a** at 540 nm showed a clean first-order decay with a rate constant of  $(4.02 \pm 0.2) \times 10^{-2} \text{ M}^{-1} \text{ s}^{-1}$ . This corresponds to  $\Delta G^\ddagger = 19.2 \pm 1.0 \text{ kcal/mol}$  (see Supporting Information, Figures S1 and S2, for details).

Since tetrazine cycloadditions are generally inverse electron demand Diels–Alder reactions, it was anticipated that a more electron deficient tetrazine would react faster. The ynamine **2a** has previously been shown to be an effective dienophile.<sup>1c,h</sup> The faster the cycloaddition reaction, the lower the upper limit for the deazetization and hence the lower the barrier. Indeed, the tetrazine diester **1b** and the ynamine **2a** reacted instantaneously upon mixing and gave the corresponding pyridazine **4b** in quantitative yield. This reaction was too fast to follow with a conventional UV spectrophotometer but proved amenable to study using a stopped-flow spectrophotometer.



**Stopped-Flow Kinetic Studies.** The disappearance of tetrazine diester **1b** ( $3.1 \times 10^{-3}$  M in dioxane after mixing) at various concentrations of ynamine **2a** was monitored in a stopped-flow spectrometer at 288.2 K. At an equal concentration of **2a**, a time-dependent absorption spectra was obtained, which showed a clear isosbestic point at 428 nm (Figure 2). With the ynamine **2a** in pseudo-first-order excess (0.046–0.196 M in dioxane after mixing), the kinetics of the disappearance of **1b** was monitored at the  $\lambda_{\text{max}}$  of 520 nm. This gave a rate constant of  $(1.11 \pm 0.11) \times 10^4 \text{ M}^{-1} \text{ s}^{-1}$  and a  $\Delta G^\ddagger$  of  $11.5 \pm 1.2 \text{ kcal/mol}$  for the cycloaddition.

The absorbance at 428 nm was also monitored under these conditions (Figure 3); there was no change in the absorbance, again indicating the presence of an isosbestic point. The assumption is made that the putative bicyclic intermediate **3b**

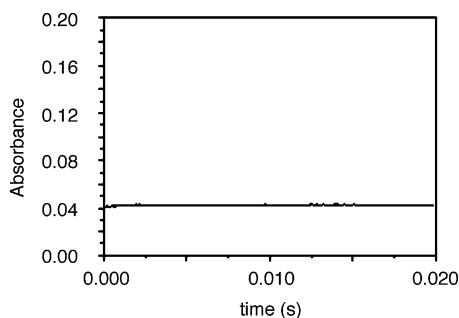


**Figure 3.** Time evolution of the absorption at the isosbestic point (428 nm) of 1:25 ratio of tetrazine diester (**1b**,  $3.1 \times 10^{-3}$  M in dioxane after mixing) vs ynamine (**2a**,  $7.7 \times 10^{-2}$  M in dioxane) at 15 °C.

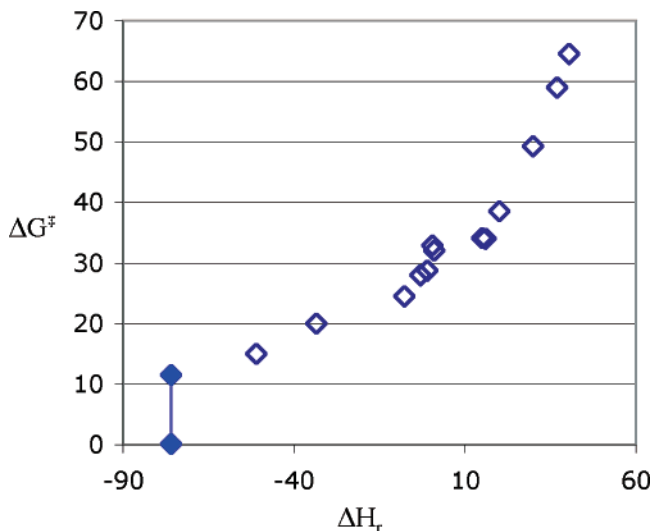


**Figure 4.** Correlation of  $\Delta H_r$  with  $\Delta G^\ddagger$  (kcal/mol). Open diamonds are from Berson's correlation,<sup>3</sup> and the filled diamonds represent the possible range of the barrier for deazetization of **3b** from this work. (See Table S4 for data.)

would not absorb at the isosbestic point.<sup>11</sup> Thus an accumulation of **3b** should lead to a decrease in absorbance at 428 nm. In Figure 3, even a 10% decrease in absorbance would be clearly visible; thus the concentration of **3b** can never be more than 10% of the initial concentration of **1b**.

Even at the highest concentration of **2a** (0.196 M), no decrease in the absorption at the isosbestic point was observed. Furthermore, the reaction was complete within the mixing time of the stopped-flow apparatus; there would be no further advantage for a faster reaction. Numerical integration of rate constants (see Supporting Information for details) requires that the intermediate must decompose with a rate constant at least four times faster than the extrapolated  $k_{\text{obs}}$  for the Diels–Alder cycloaddition at this concentration. This corresponds to a rate constant of  $(8.8 \pm 2.0) \times 10^3 \text{ M}^{-1} \text{ s}^{-1}$  and a  $\Delta G^\ddagger$  of  $11.6 \pm 2.6$  kcal/mol for the loss of  $\text{N}_2$ . The free energy of activation for the loss of nitrogen from **3b** must be lower than this! Figure 4 extends Berson's correlation<sup>3</sup> to include this new data. Following Berson, the  $\Delta H_r$  for the reaction of **3b** was calculated from Benson's additivity tables.<sup>3d</sup>

**Computational Results.** How low is the barrier for loss of  $\text{N}_2$ ? First, the parent reaction between 1,2,4,5-tetrazine (**1c**) and ethyne (**2b**) was examined at several levels of theory. The B3LYP/6-31G(d,p)<sup>12</sup> method has been widely applied and shown to be reasonably accurate for the calculation of concerted, pericyclic organic reactions.<sup>13</sup> The 6-311+G(2d,2p) basis set was also used. The MP2/6-31G(d,p) method was also used in this work; it has also been widely applied, but it has been shown

to underestimate barrier heights in some pericyclic reactions.<sup>13c,d</sup> Additionally, two model reactions with electron-deficient substituents on the tetrazine (**1d**,  $\text{R} = \text{CO}_2\text{H}$  and **1e**,  $\text{R} = \text{CF}_3$ ) with an electron-rich alkyne (**2c**) were also studied. The starting materials, transition structures, intermediates, and products were optimized using Gaussian 98<sup>14</sup> along the anticipated reaction coordinate. The transition structures and minima were characterized by frequency calculations and had one or zero imaginary frequencies, respectively. Two conformations of the acid substituents (**1d** and **1d'**) were considered. For the trifluoromethyl system (**1e**), the two regioisomers of the second addition of ethynylamine to **4e** were also considered. Energy values of reactants, products, and transition structures are shown in Tables 1–4 and shown graphically in Figures 5–7.

Initial studies of the parent reaction found a well-defined transition structure (**TS1c**) for the addition of ethyne (**2b**) to tetrazine (**1c**) at the three levels of theory. However, the existence of the intermediate **3c** is precarious at best. At the B3LYP/6-31G(d,p) level of theory, **3c** is a properly characterized minimum. However, the barrier for loss of  $\text{N}_2$  (via **TS2c**) is calculated to be only 0.24 kcal/mol, once the zero-point vibrational energy (ZPVE) corrections are made. As would be expected<sup>2,3</sup> for such an exothermic reaction ( $-65.1$  kcal/mol, calculated), this is a very early transition structure, with the breaking C–N bonds only 0.125 Å longer in **TS2c** than in **3c**. With a larger basis set (B3LYP/6-311+G(2d,2p)) there is a small barrier of 0.61 kcal/mol on the Born–Oppenheimer potential energy surface (PES), but once the ZPVE correction is made, there is no barrier for loss of nitrogen. Although **3c** is not a transition structure, it is calculated to be a transition state.<sup>15</sup> Thus, the reaction from **1c** and **2b** to **4c** is calculated to proceed via two sequential transition states, as shown in Figure 1.

Furthermore, at the MP2/6-31G(d,p) level, the symmetrical structure **3c** is not a minimum but a transition structure on the PES. The reaction coordinate corresponds to loss of either nitrogen. The exothermicity of the reaction from **3c** to **4c** is apparently sufficient to make the barrier corresponding to **TS2c** vanish. Therefore, at this level of theory at least, the PES has two sequential transition structures.

The reaction of the tetrazinediacid **1d** with ethynylamine (**2c**) was computed as a model system for the experimental reaction of **1b** with **2a** (Table 2 and Figure 5). The B3LYP/6-31G(d,p) + ZPVE level is a conservative choice of method; based on the results for **1c** above, it is more likely to find a barrier for loss of  $\text{N}_2$ . Two conformations of the acid groups were considered for **1d**, with the carbonyls on the same or opposite sides of the tetrazine ring. The lower of the two transition structures (**TS1d**) for the initial Diels–Alder cycloaddition of **1d** with **2c** was calculated to be concerted but very asynchronous; the forming bonds are 1.892 and 2.944 Å. The barrier for the reaction via **TS1b** is 7.6 kcal/mol. This barrier cannot be directly compared to the experimental  $\Delta G^\ddagger$  of  $11.5 \pm 1.2$  kcal/mol for the cycloaddition of **1b** with **2a**. However, if one assumes a typical value of  $-34$  eu for  $\Delta S^\ddagger$  for a bimolecular Diels–Alder,<sup>16</sup> this suggests an experimental value of  $\Delta H^\ddagger$  of approximately 1.7 kcal/mol at 15 °C, which is not too far from the calculated barrier of 7.6 kcal/mol.

The adduct **3d** is calculated to be a true intermediate, albeit with a barrier of only 1.5 kcal/mol (after the ZPVE correction) for loss of one of the nitrogens via the synchronous transition structure **TS2d**. Given the computational results for **3c** above, it is possible that at the MP2/6-31G(d,p) level there might not be a barrier. Either a low or a nonexistent barrier would be

**TABLE 1: Relative Energies (RE, kcal/mol), RE with Zero-Point Vibrational Energies (ZPVE) Corrections, and Low or Imaginary Frequencies ( $\text{cm}^{-1}$ ) for the Reaction of **1c** with **2b** at Various Levels of Theory**

	B3LYP/6-31G(d,p)			B3LYP/6-311+G(2d,2p)			MP2/6-31G(d,p)		
	RE	RE + ZPVE	low freq	RE	RE + ZPVE	low freq	RE	RE + ZPVE	low freq
<b>1c</b> + <b>2b</b>	40.31	35.69		32.84	28.53		44.63	40.42	
<b>TS1c</b>	58.24	55.09	498.6i	54.67	51.74	516.1i	56.23	53.79	446.8i
<b>3c</b>	0.0	0.0	377.4	0.0	0.0	341.7	<b>0.0<sup>a</sup></b>	<b>0.0<sup>a</sup></b>	<b>235.8i</b>
<b>TS2c</b>	0.93	0.24	415.5i	0.61	<b>-0.001</b>	389.1i			
<b>4c</b> + $\text{N}_2$	-62.81	-65.11		-68.49	-70.74		-67.32	-69.31	

<sup>a</sup> Note that **3c** is a transition structure at the MP2/6-31G(d,p) level of theory.

**TABLE 2: B3LYP/6-31G(d,p) Relative Energies (RE, kcal/mol), RE with Zero-Point Vibrational Energies (ZPVE) Corrections, and Low or Imaginary Frequencies ( $\text{cm}^{-1}$ )<sup>a</sup>**

	RE	RE + ZPVE	low freq
<b>1d</b> + <b>2c</b>	44.6	41.0	
<b>1d'</b> + <b>2c</b>	44.7	41.1	
<b>TS1d</b>	50.5	48.6	300.7i
<b>TS1d'</b>	51.4	49.5	282.9i
<b>3d</b>	0.0	0.0	31.3
<b>TS2d</b>	1.5	1.5	42.5i
<b>4d</b> + $\text{N}_2$	-74.3	-75.6	

<sup>a</sup> **1d'**, **TS1d'**, and **TS2d'** correspond to alternative conformations. The frequencies of **1d**, **1d'**, **2d**,  $\text{N}_2$ , and **4d** are 15.8, 16.4, 346.9, 2457.7, and 24.8  $\text{cm}^{-1}$ , respectively.

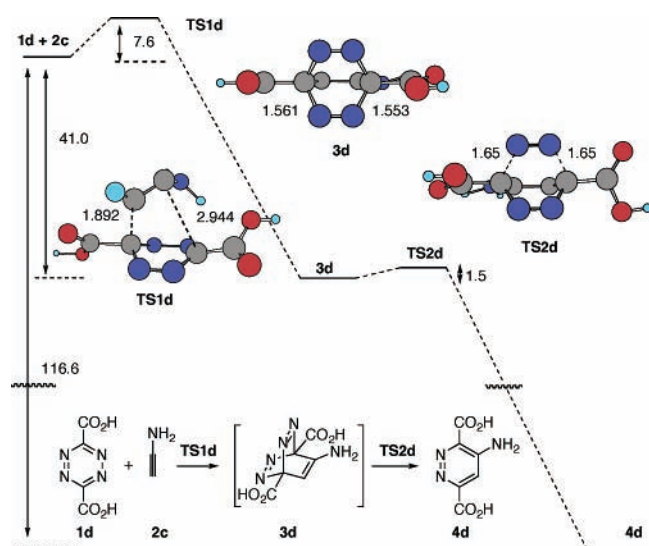


**Figure 5.** Relative energies (kcal/mol) and selected optimized geometries for the reaction of **1d** with **2c**, calculated at the B3LYP/6-31G(d,p) + ZPVE level. Distances in Angstroms. Carbon, black; nitrogen, blue; oxygen, red; hydrogen, green.

consistent with the experimental result that the barrier for loss of nitrogen from **3b** must be lower than  $11.6 \pm 2.6$  kcal/mol.

The trifluoromethyl groups in **1e** would be expected to be even more inductively electron withdrawing than the acids of **1d**. In part to see if there would be an experimental advantage to using **1e** and in part to see what effects the trifluoromethyl groups might have, the reaction sequence **1e** to **4e** was calculated (Table 3 and Figure 6). The transition structure (**TS1e**) for the cycloaddition of **1e** with **2c** is again calculated to be concerted but asynchronous. The barrier height is reduced somewhat (4.4 kcal/mol) as compared to the diacid (**1d**, 7.6 kcal/mol). Because the kinetic experiments are limited by the mixing time, the more rapid cycloaddition would not provide a significant experimental advantage, so the multistep synthesis of **1e** was not repeated.<sup>17</sup> A very shallow minimum corresponding to **3e** was located as well as a transition structure for loss of  $\text{N}_2$ . However, after

**TABLE 3: B3LYP/6-31G(d,p) Relative Energies (RE, kcal/mol), RE with Zero-Point Vibrational Energies (ZPVE) Corrections, and Low or Imaginary Frequencies ( $\text{cm}^{-1}$ ) for the Reaction of **1e** with **2c**<sup>a</sup>**

	RE	RE + ZPVE	low freq
<b>1e</b> + <b>2c</b>	48.1	44.2	
<b>TS1e</b>	51.0	48.6	265.4 i
<b>3e</b>	0.0	0.0	47.3
<b>TS2e</b>	0.6	0.1	349.3i
<b>4e</b> + $\text{N}_2$	-69.7	-71.4	

<sup>a</sup> The frequency of **1e** is 5.0  $\text{cm}^{-1}$  and of **4e** is 21.5  $\text{cm}^{-1}$ .

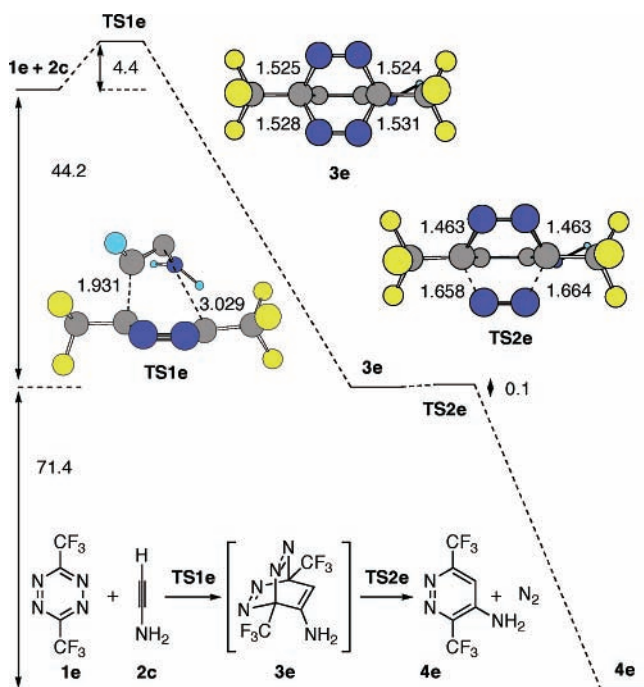


**Figure 6.** Relative energies and selected optimized geometries for the reaction of **1e** and **2c**, at the B3LYP/6-31G(d,p) + ZPVE level. Fluorine, yellow; see Figure 5 for key.

correction for the ZPVE, this barrier essentially vanishes (0.1 kcal/mol). The reaction may also have two sequential transition states.

For these substituents, the second Diels–Alder reaction between pyridazine **4e** and ynamine **2c** was also calculated (Table 4 and Figure 7). The barrier of 29.2 kcal/mol is consistent with the experimental result that the pyridazines **4a** and **4b** do not undergo this cycloaddition but are isolated under the experimental reaction conditions. Significantly, the intermediate **5e** and the transition structure **TS4e** could not be located in our calculations at this level of theory. In one sense, this is not at all surprising; as above, the loss of  $\text{N}_2$  to form an aromatic ring is extremely exothermic; thus, the barrier might well be nonexistent. However, this actually presents a problem in the description of the reaction. When there are two molecules of

**TABLE 4: B3LYP/6-31G(d,p) Relative Energies (RE, kcal/mol), RE with Zero-Point Vibrational Energies (ZPVE) Corrections, and Low or Imaginary Frequencies ( $\text{cm}^{-1}$ ) for the Reaction of **4e** with **2c**, **TS3e'**, and **6e'** Correspond to the Regioisomers of the Second Adduct Transition Structure and Final Product, Respectively<sup>a</sup>**

name	RE	RE + ZPVE	low freq
<b>4e</b> + <b>2c</b>	0.0	0.0	
<b>TS3e</b>	28.2	29.3	262.2i
<b>TS3e'</b>	27.5	28.7	226.2i
<b>5e<sup>b</sup></b>			
<b>TS4e<sup>b</sup></b>			
<b>6e</b> + $\text{N}_2$	-100.4	-76.1	
<b>6e'</b> + $\text{N}_2$	-100.5	-76.3	

<sup>a</sup> The frequencies of **4e**, **6e**, and **6e'** are 21.5, 37.1, and 16.0  $\text{cm}^{-1}$ , respectively. <sup>b</sup> Structures corresponding to **5e** and **TS4e** could not be located.

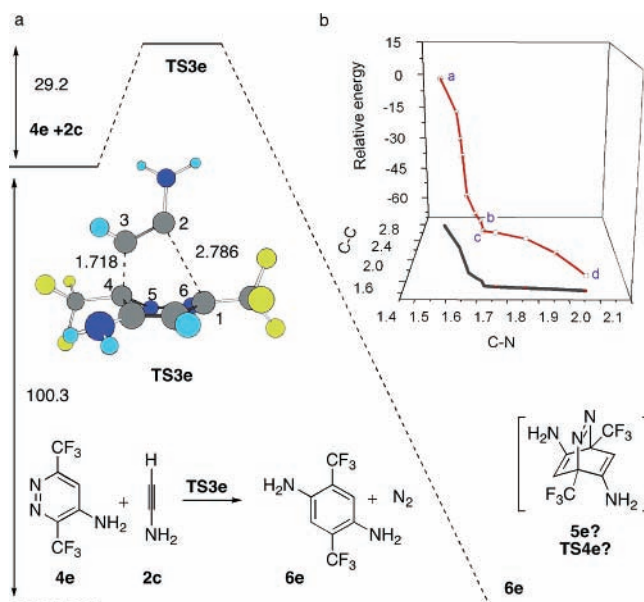


**Figure 7.** (a) Relative energies and optimized TS geometry for the reaction of **4e** and **2c**, at the B3LYP/6-31G(d,p) + ZPVE level. See Figure 5 for key. (b) Relative energies of constrained optimizations along the reaction coordinate. See text for discussion and Table S6 for the distances and energies.

nitrogen that can leave without a barrier, the symmetry of the system means there is a transition structure. But there is no similar mathematically well-defined point corresponding to **5e**, although the PES structure corresponds to a reasonable Lewis dot structure. Figure 7b shows the relative energies from constrained optimizations, approximating the IRC. Point a is **TS3e**. From point a to b, only the C1–C2 distance was fixed, and the C4–N5 (longer) bond is plotted. Attempted optimization at C1–C2 distances shorter than 1.61 Å led to loss of  $\text{N}_2$ . Points c to d had both C1–N6 and C4–N5 fixed at equal distances, and the C1–C2 bond is plotted. If one considers skiing as analogous to going down a PES, it is as if the reaction turns a corner at points b and c. Furthermore, it appears that there is chemical significance to this corner. In the Bell–Evans–Polanyi Principle/Hammond Postulate/Berson correlation sense,<sup>2,3</sup> the initial Diels–Alder transition structure **TS3e** does not feel the full exothermicity of the overall reaction to form **6e**; if it did, there would be no barrier for this cycloaddition. Rather, it would seem that the modest barrier to **TS3e** reflects the exothermicity only to **5e**.

## Conclusions

The rate of the Diels–Alder cycloadditions of *N,N*-diethyl-1-propynylamine (**2a**) with diphenyltetrazine (**1a**) in dioxane at room temperature was monitored by UV and gives  $\Delta G^\ddagger = 19.2 \pm 1.0$  kcal/mol. The reaction of **2a** with **1b** is faster, requiring the use of stopped-flow techniques to measure the rate. This gave  $\Delta G^\ddagger = 11.5 \pm 1.2$  kcal/mol. Both reactions showed clear isosbestic points; for the reaction of **2a** with **1b**, this places an upper limit of  $11.6 \pm 2.6$  kcal/mol on  $\Delta G^\ddagger$  for loss of  $\text{N}_2$  from the putative bicyclic intermediate **3b**. Calculations of transition structures for the parent reaction of **1c** with **2b** predict that there may be no barrier for the loss of nitrogen from **3c**. This means that there are two sequential transition states on the energy surface, the first for the Diels–Alder (**TS1c**) and the second corresponding to formal  $\text{N}_2$  substitution (**3c**). As a closer model system, the reaction of tetrazinediacid **1d** with propynylamine **2c** was calculated. At the B3LYP/6-31G(d,p) + ZPVE level, the barrier for the cycloaddition via **TS1d** is calculated to be 7.6 kcal/mol, while there is only a very small barrier of 1.5 kcal/mol for loss of  $\text{N}_2$  from **3d** via **TS2d**. Both of these calculated energies are consistent with the experimental results for the reaction of **1b** with **2a**. Whether the barrier for loss of  $\text{N}_2$  is  $11.6 \pm 2.6$  kcal/mol or is nonexistent, Berson's correlation of activation energy with reaction energy in pericyclic reactions is extended to significantly lower barriers. It appears that a sufficiently exothermic pericyclic fragmentation will not have a barrier.

Similar calculations for the reactions of the more electro-negative bis-trifluoromethyltetrazine **1e** predict even lower barriers for the initial cycloaddition via **TS1e** (4.4 kcal/mol) and for the loss of  $\text{N}_2$  from **3e** (0.1 kcal/mol). The calculated barrier for a second cycloaddition to **4e** via **TS3e** is calculated to be 29.2 kcal/mol, consistent with the experimental observation that pyridazines **4** do not react with alkynes at room temperature. Interestingly, past **TS3e**, there is not an intermediate or transition state before the final product **6e**. It appears that the energy surface turns a corner in the vicinity of a structure resembling **5e**. This is not mathematically well-defined but has chemical consequences in that the overall exothermicity of the reaction from **4e** to **6e** is not felt in **TS3e**.

## Experimental Section

**Synthesis.** Dioxane was freshly distilled over calcium hydride. 3,6-Dicarbomethoxy-1,2,4,5-tetrazine (**1b**) was synthesized using the procedure of Boger et al.<sup>1d</sup> *N,N*-Diethyl-1-propynylamine (**2b**) was synthesized by isomerization of *N,N*-diethylpropargylamine using the procedure described by Mandesa.<sup>18</sup> <sup>1</sup>H NMR (300 MHz,  $\text{CDCl}_3$ ):  $\delta$  2.81(q,  $J = 7.2$  Hz, 4H), 1.88 (s, 3H), 1.15 (t,  $J = 7.2$  Hz, 6H).

**UV Studies of 3,6-Diphenyl-1,2,4,5-tetrazine (1a) and *N,N*-Diethyl-1-propynylamine (2a).** UV–Vis experiments were performed on a Shimadzu UV-1601 UV–Vis spectrophotometer controlled by UV Probe (version 1.11) software. The reaction of 3,6-diphenyl-1,2,4,5-tetrazine (**1a**) with *N,N*-diethyl-1-propynylamine (**2a**) was performed at room temperature in the UV–Vis spectrophotometer. Tetrazine **1a** (2.0 mg, 8.5  $\mu\text{mol}$ ) was dissolved in 10 mL of a mixture of dioxane and acetonitrile (5:1) to give a final concentration of 1.0 mM. A portion of this solution (3.5 mL, 2.9  $\mu\text{mol}$  of diphenyltetrazine) was added to a cuvette, and the UV absorption was recorded. Ynamine **2a** (20  $\mu\text{L}$ , 0.14 mmol, 50 equiv) was added in one portion, and the mixture was shaken briefly. A series of UV spectra were recorded every 30 s for 15 min. Under these conditions, the reaction showed a clean pseudo-first-order-decay at the absorp-

tion maxima of **1a** ( $\lambda_{\max}$  540 nm, molar absorptivity  $\epsilon = 2.7 \times 10^4$ ) and also an isosbestic point at 448 nm (see Supporting Information Figure S1). A plot of absorbance versus time was fit with a first-order exponential decay. The rate from this graph is shown in the Figure S2. The reaction mixture was rotavaped to isolate the adduct from excess ynamine (**2a**) and solvents; NMR of the crude reaction mixture showed quantitative conversion to 3,6-diphenyl-4-(*N,N*-diethylamino)-5-methylpyridazine (**4a**). It was purified by column chromatography on silica gel using 2:8 EtOAc: hexane to give **4a**. <sup>1</sup>H NMR (500 MHz, CDCl<sub>3</sub>):  $\delta$  7.70 (dm,  $J = 7.0$ , 2H), 7.65 (dm,  $J = 7.0$ , 2H), 7.42–7.52 (m, 6H), 2.96 (q,  $J = 7.0$ , 4H), 2.25 (s, 3H), 1.02 (t,  $J = 7.0$ , 6H). <sup>13</sup>C NMR (500 MHz, CDCl<sub>3</sub>)  $\delta$  162.0, 157.2, 147.6, 138.6, 138, 131.4, 129.6, 128.8, 128.5, 128.27, 128.25, 128.22, 46.1, 17.4, 13.7. (The preparation of **4a** has previously been reported<sup>1c</sup>.)

**3,6-Dicarbomethoxy-4-(*N,N*-diethylamino)-5-methylpyridazine (**4b**).** To a solution of 0.026 g (0.13 mmol) of 3,6-dicarbomethoxy-1,2,4,5-tetrazine (**1b**) in dry dioxane at room temperature was slowly added a solution of 18  $\mu$ L (0.13 mmol) of *N,N*-diethyl-1-propynylamine (**2a**). An immediate reaction occurred. The bright red color of the tetrazine disappeared, and a pale yellow solution was obtained. The reaction mixture was rotavaped to isolate the adduct from excess ynamine and solvents. The conversion to **4b** was quantitative by NMR. The reaction mixture was purified by column chromatography on silica gel using 2:8 EtOAc:hexane to give **4b**. <sup>1</sup>H NMR (500 MHz, CDCl<sub>3</sub>):  $\delta$  4.02 (s, 3H), 4.01 (s, 3H), 3.17 (q,  $J = 7$ , 4H), 2.36 (s, 3H), 1.09 (t,  $J = 7$ , 3H). <sup>13</sup>C NMR (500 MHz, CDCl<sub>3</sub>)  $\delta$  166.2, 165.8, 154.4, 151.5, 148.3, 133.5, 53.2, 53.1, 45.8, 29.6, 15.0, 13.4. (The preparation of the hydrochloride salt of **4b** has previously been reported.<sup>1c</sup>)

**Stopped-Flow Studies on the Reaction of 1b with 2a.** Kinetic experiments in dioxane were performed with a computer-controlled SX-18 MV stopped-flow reaction spectrophotometer (Applied Photo Physics Ltd. Surrey, U.K.). The cell box and the drive syringes of the stopped-flow reaction analyzer were flushed a minimum of three times with dry solvents to make the system oxygen-free. A stock solution of 3,6-dicarbomethoxy-1,2,4,5-tetrazine (**1b**,  $6.1 \times 10^{-3}$  M in dioxane) was prepared. Solutions of the ynamine (**2a**) (0.092 M to 0.40 M in dioxane) were in high concentration relative to **1b** to maintain pseudo-first-order conditions. The tetrazine **1b** and ynamine **2a** solutions were taken separately in airtight syringes from a drybox and injected in equal volumes into the stopped-flow system. Pseudo-first-order reaction rate constants were determined from the decay of the tetrazine **1b** monitored at 520 nm. (See Figures S3 and S4.)

**Acknowledgment.** Financial support of this work from the National Science Foundation (CHE-0415622) (D.V.S. and D.M.B.), (CHE-0413845) (R.A.F.) and from the Robert A. Welch Foundation (D.V.S. and D.M.B.) is gratefully acknowledged.

**Supporting Information Available:** Representative figures of absorbance versus time for reactions **1a** and **1b**,  $k_{\text{obs}}$  versus [2a] for stopped-flow experiments, numerical integration of rate constants, absolute energies and Cartesian coordinates for all stationary points. This material is available free of charge via the Internet at <http://pubs.acs.org>.

## References and Notes

- (1) (a) Boger, D. L.; Weinreb, S. M. *Hetero Diels–Alder Methodology in Organic Synthesis*; Academic: San Diego, 1987. (b) Sauer, J. *Comprehensive Heterocyclic Chemistry II*; Pergamon: London, 1996; Vol. 6, pp 901–965. (c) Roffey, P.; Verge, J. P. *J. Heterocycl. Chem.* **1969**, *6*, 497–502. (d) Boger, D. L.; Coleman, R. S.; Panek, J. P.; Huber, F. X.; Sauer, J. *J. Org. Chem.* **1985**, *50*, 5377–5379. (e) Warren, R. N.; Margetic, D.; Amarasekara, A. S.; Butler, D. N.; Mahadevan, I. B.; Russell, R. A. *Org. Lett.* **1999**, *1*, 199–202. (f) Warren, R. N.; Harrison, P. A. *Molecules* **2001**, *6*, 353–369. (g) Bodwell, G. J.; Li, J. *Org. Lett.* **2002**, *4*, 127–130. (h) Soenen, D. R.; Zimpleman, J. M.; Boger, D. L. *J. Org. Chem.* **2003**, *68*, 3593–3598. (i) Yeung, B. K. S.; Boger, D. L. *J. Org. Chem.* **2003**, *68*, 5249–5253.
- (2) Such a correlation is implicit in the Hammond Postulate (a) and is explicit in the Bell–Evans–Polanyi Principle (b and c). A more comprehensive view is Jenks' Bema Hypothesis (d). (a) Hammond, G. S. *J. Am. Chem. Soc.* **1955**, *77*, 334. (b) Bell, R. P. *Proc. R. Soc. London, Ser. A* **1936**, *154*, 414. (c) Evans, M. G.; Polanyi, M. *Trans. Faraday Soc.* **1938**, *34*, 11–29. (d) Jenks, W. P. *Chem. Rev.* **1985**, *86* (6), 511–527.
- (3) (a) Birney, D. M.; Berson, J. A. *Tetrahedron* **1986**, *42*, 1561–1570. (b) Birney, D. M.; Berson, J. A. *J. Am. Chem. Soc.* **1985**, *107*, 4553–4554. (c) Birney, D. M.; Ham, S.; Unruh, G. R. *J. Am. Chem. Soc.* **1997**, *119*, 4509–4517. (d) Benson, S. W.; Cruickshank, F. R.; Golden, D. M.; Haugen, G. R.; O'Neil, A. E.; Rogers, A. S.; Shaw, R.; Walsh, R. *Chem. Rev.* **1969**, *69*, 279–324.
- (4) Marcus, R. A. *J. Phys. Chem.* **1968**, *72*, 891–899.
- (5) (a) Murrell, J. N.; Laidler, K. J. *Trans. Faraday Soc.* **1968**, *64*, 371–377. (b) McIver, J. W. *Acc. Chem. Res.* **1974**, *7*, 72–77. (c) Stanton, R. E.; McIver, J. W., Jr. *J. Am. Chem. Soc.* **1975**, *97*, 3632–3646.
- (6) The IRC was originally defined by Fukui (a). As implemented in Gaussian (b) a steepest descent in mass-weighted internal coordinates will not break symmetry. For a discussion, see ref 7f. (a) Fukui, K. *Acc. Chem. Res.* **1981**, *14*, 363–368. (b) González, C.; Schlegel, H. B. *J. Phys. Chem.* **1990**, *94*, 5523.
- (7) One of the earliest discussions of valleys and ridges on potential energy surfaces appears to have been by (a) Metiu, H.; Ross, J.; Silbey, R.; George, T. F. *J. Chem. Phys.* **1974**, *61*, 3200–3209. The valley–ridge inflection point has been extensively discussed by Ruedenberg et al. (b) Valtazanos, P.; Elbert, S. F.; Ruedenberg, K. *J. Am. Chem. Soc.* **1986**, *108*, 3147–3149. (c) Xantheas, S.; Valtazanos, P.; Ruedenberg, K. *Theor. Chim. Acta* **1991**, *78*, 327–363. More recent discussions and applications include (d) Hirsch, M.; Quapp, W.; Heidrich, D. *Phys. Chem. Chem. Phys.* **1999**, *1*, 5291. (e) Kumeda, Y.; Taketsugu, T. *J. Chem. Phys.* **2000**, *113*, 477. For an excellent, detailed overview of the features of PESS, see (f) Wales, D. J. *Energy Landscapes*; Cambridge University Press: Cambridge, 2003.
- (8) (a) Lyons, B. A.; Pfeifer, J.; Peterson, T. H.; Carpenter, B. K. *J. Am. Chem. Soc.* **1993**, *115*, 2427–2437. (b) Reyes, M. B.; Carpenter, B. K. *J. Am. Chem. Soc.* **2000**, *122*, 10163–10176. (c) Adam, W.; Grüne, M.; Diederich, M.; Trofimov, A. V. *J. Am. Chem. Soc.* **2001**, *123*, 7109–7112.
- (9) (a) Bartsch, R. A.; Chae, Y. M.; Ham, S.; Birney, D. M. *J. Am. Chem. Soc.* **2001**, *123*, 7479–7486. (b) Mann, D. J.; Hase, W. L. *J. Am. Chem. Soc.* **2002**, *124*, 3208–3209. (c) Castaño, O.; Palmeiro, R.; Frutos, L. M.; Luisandrés, J. *J. Comput. Chem.* **2002**, *23*, 732–735. (d) Reyes, M. B.; Lobkovsky, E. B.; Carpenter, B. K. *J. Am. Chem. Soc.* **2002**, *124*, 641–651. (e) Debbert, S. L.; Carpenter, B. K.; Hrovat, D. A.; Borden, W. T. *J. Am. Chem. Soc.* **2002**, *124*, 7896–7897. (f) Zhou, C.; Birney, D. M. *Org. Lett.* **2002**, *4* (19), 3279–3282. (g) Suh rada, C. P.; Selçuki, C.; Nendel, N.; Cannizzaro, C.; Houk, K. N.; Rissing, P.-J.; Baumann, D.; Hasselmann, D. *Angew. Chem. Int. Ed.* **2005**, *44*, 3548–3552.
- (10) (a) Toma, L.; Romano, S.; Quadrelli, P.; Caramella, P. *Tetrahedron Lett.* **2001**, *42*, 5077–5080. (b) Caramella, P.; Quadrelli, P.; Toma, L. *J. Am. Chem. Soc.* **2002**, *124*, 1130–1131.
- (11) 1-Methyl-2,3-diazabicyclo[2.2.2]oct-2-ene ( $\lambda_{\max}$  380 nm,  $\epsilon$  200) could serve as a model compound for the UV absorption of the diaza moiety of **3b**. Engel, P. S.; Hayes, R. A.; Keifer, L.; Szilagyi, S.; Timberlake, J. W. *J. Am. Chem. Soc.* **1978**, *100*, 1876–1882.
- (12) (a) Becke, A. D. *J. Chem. Phys.* **1993**, *98*, 5648–5652. (b) Stephens, P. J.; Devlin, F. J.; Chabalowski, C. F.; Frisch, M. J. *J. Chem. Phys.* **1994**, *98*, 11623–11627. (c) Hariharan, P. C.; Pople, J. A. *Theor. Chim. Acta* **1973**, *28*, 213.
- (13) (a) Petersson, G. A.; Malick, D. K.; Wilson, W. G.; Ochterski, J. W.; Montgomery, J. A.; Frisch, M. J. *J. Chem. Phys.* **1998**, *109*, 10570–10579. (b) Ochterski, J. W.; Petersson, G. A.; Wiberg, K. B. A Comparison of Model Chemistries. *J. Am. Chem. Soc.* **1995**, *117*, 11299–11308. (c) Wiest, O.; Montiel, D. C.; Houk, K. N. *J. Phys. Chem. A* **1997**, *101*, 8378–8388. (d) Birney, D. M. *J. Am. Chem. Soc.* **2000**, *122*, 10917–10925.
- (14) Frisch, M. J.; Trucks, G. W.; Schlegel, H. B.; Scuseria, G. E.; Robb, M. A.; Cheeseman, J. R.; Zakrzewski, V. G.; Montgomery, J. A., Jr.; Stratmann, R. E.; Burant, J. C.; Dapprich, S.; Millam, J. M.; Daniels, A. D.; Kudin, K. N.; Strain, M. C.; Farkas, O.; Tomasi, J.; Barone, V.; Cossi, M.; Cammi, R.; Mennucci, B.; Pomelli, C.; Adamo, C.; Clifford, S.; Ochterski, J.; Petersson, G. A.; Ayala, P. Y.; Cui, Q.; Morokuma, K.; Malick, D. K.; Rabuck, A. D.; Raghavachari, K.; Foresman, J. B.; Cioslowski, J.; Ortiz, J. V.; Stefanov, B. B.; Liu, G.; Liashenko, A.; Piskorz, P.; Komaromi,

I.; Gomperts, R.; Martin, R. L.; Fox, D. J.; Keith, T.; Al-Laham, M. A.; Peng, C. Y.; Nanayakkara, A.; Gonzalez, C.; Challacombe, M.; Gill, P. M. W.; Johnson, B. G.; Chen, W.; Wong, M. W.; Andres, J. L.; Head-Gordon, M.; Replogle, E. S.; Pople, J. A. *Gaussian 98*, revision A.6; Gaussian, Inc.: Pittsburgh, PA, 1998.

(15) We use "transition structure" in reference to the Born–Oppenheimer potential energy surface and "transition state" in reference to the energy surface with ZPVE corrections. Houk, K. N.; Li, Y.; Evansck, J. D. *Angew. Chem., Int. Ed. Engl.* **1992**, *31*, 682–708.

(16)  $\Delta S^\ddagger$  values for Diels–Alder reactions of various dienes and dienophiles range from  $-40$  to  $-22$  e.u. in a range of solvents. Sauer, J.; Sustmann, R. *Angew. Chem. Int. Ed. Engl.* **1980**, *19*, 779–807.

(17) (a) Brown, H. C.; Cheng, M. T.; Parcell, L. J.; Pilipovich, D. *J. Org. Chem.* **1961**, *26*, 4407–4409. (b) Barlow, M. G.; Haszeldine, R. N.; Pickett, J. A. *J. Chem. Soc., Perkin Trans. 1* **1978**, 378–380.

(18) Mandesa, L. *Preparative Acetylenic Chemistry*, 2nd ed.; Elsevier Science Publishers, Amsterdam, 1988.